N87-20536

# ALUMINA-SUPPORTED Pd-Ag CATALYSTS FOR LOW-TEMPERATURE CO AND METHANOL OXIDATION

R. W. McCabe
Physical Chemistry Department
General Motors Research Laboratories
Warren, Michigan

## ABSTRACT

Pd-Ag bimetallic catalysts, supported on $\gamma$-$Al_2O_3$, have been evaluated as exhaust catalysts for methanol-fueled vehicles. Laboratory studies have shown that a 0.01% Pd-5% Ag catalyst has greater CO and $CH_3OH$ oxidation activity than either 0.01% Pd or 5% Ag catalysts alone. Moreover, Pd and Ag interact synergistically in the bimetallic catalyst to produce greater CO and $CH_3OH$ oxidation rates and lower yields of methanol partial oxidation products than expected from a mixture of the single-component catalysts. The Pd-Ag synergism results from Pd promoting the rate of $O_2$ adsorption and reaction with CO and $CH_3OH$ on Ag. Rate enhancement by the bimetallic catalyst is greatest at short reactor residence times where the oxygen adsorption rate limits the overall reaction rate.

## INTRODUCTION

Methanol-fueled vehicles differ greatly from gasoline vehicles in their exhaust characteristics. Major differences include the absence of sulfur in methanol exhaust and much lower exhaust temperatures associated with methanol vehicles. The latter provides impetus for developing catalysts that are effective for low-temperature CO and $CH_3OH$ oxidation.

This study is part of a continuing effort in our laboratory to develop catalysts specifically for methanol-fueled vehicles. We begin by reviewing our previous results obtained with single-component catalysts. Those experiments suggested the use of bimetallic catalysts, and this paper focuses on results obtained with a bimetallic Pd-Ag/$\gamma$-$Al_2O_3$ catalyst.

## EXPERIMENTAL PROCEDURE

### Reactor System

The reactor and experimental methods were identical to those employed previously [1] and are only briefly reviewed here. A schematic diagram of the apparatus is shown in Fig. 1. The reactor was a 2.5 cm o.d. quartz tube

PRECEDING PAGE BLANK NOT FILMED

housed in a single-zone furnace. The feed gases passed downward through the reactor and sequentially contacted stacked layers of (1) quartz beads (for preheating and feed), (2) the catalyst pellets, and (3) quartz wool (for supporting the catalyst and quartz beads). Temperatures were measured with a chromel-alumel thermocouple positioned along the reactor centerline with its tip located in the catalyst bed a few millimeters below the top of the bed.

Catalyst activities and selectivities were compared using three feeds: (1) 0.2% $CH_3OH$, 1% $O_2$, balance He; (2) 0.2% CO, 1% $O_2$, balance He; and (3) 0.2% $CH_3OH$, 0.2% CO, 1% $O_2$, balance He. The space velocity in most runs was 52,000 $h^{-1}$ (volume basis; standard conditions).

The products were analyzed principally with a Varian 6000 gas chromatograph equipped with both flame ionization and thermal conductivity detectors [1].

Catalysts

All catalysts were supported on 3.5 mm diameter γ-alumina beads from the same lot (Grace Chemical Co., 110 $m^2\ g^{-1}$ BET surface area, 0.5 g $cm^{-3}$ apparent bulk density).

The most notable preparative aspect of our earlier work involving a comparison of Pt, Pd, Rh, Ag, and Cu-Cr catalysts was that the noble metals Pt, Pd, and Rh were prepared and tested under conditions of equal numbers of exposed atoms and identical surface impregnation profiles [1]. In the subsequent comparison of Pd, Ag and Pd-Ag catalysts, the techniques outlined below were employed to achieve a uniform distribution of Pd and Ag throughout the interior of the pellets.

Impregnations were made from aqueous, minimum volume solutions of the metal salts - $Pd(NH_3)_4(NO_3)_2$ and $AgNO_3$. The impregnated catalysts were dried for 12 h at room temperature. The catalysts were subsequently heated in flowing air to 773 K where they were held for 4 h.

The bimetallic 0.01% Pd-5% Ag catalyst was prepared sequentially; the alumina support was first impregnated with $AgNO_3$, dried, and calcined as outlined above, and then the same procedure was repeated for the Pd ammine salt.

The 0.01% Pd catalyst has a dispersion of 42% as measured by static chemisorption at 308 K, assuming a stoichiometry of one CO molecule per exposed Pd atom. The disperson of the air-calcined 5% Ag catalyst was 27% as measured by $O_2$ chemisorption using techniques similar to those of Vannice and co-workers [2, 3]. Attempts to measure Pd-atom dispersion in the bimetallic catalyst were unsuccessful owing to difficulties in reproducibly distinguishing the small amount of irreversibly adsorbed CO associated with the Pd from the large amount of reversibly adsorbed CO associated with the Ag.

## RESULTS AND DISCUSSION

### Methanol and CO Oxidation over Selected Catalysts

Figure 2 shows steady-state methanol conversions and product yields as a function of temperature for the Pt catalyst. The Pt catalyst was extremely active and oxidized methanol even at room temperature. $CO_2$, methyl formate ($CH_3OCHO$), and $H_2CO$ were the only carbon-containing products. Methyl formate was the principal product at low temperatures, but was replaced by $CO_2$ at temperatures above 350 K.

Methanol conversion and selectivity were both greatly affected by adding CO to the feed, as shown in Fig. 3. Significant conversion of methanol was not observed below 450 K; moreover, methyl formate was no longer formed.

Similar $CH_3OH$ oxidation experiments were carried out over the Pd, Rh, Ag, and Cu-Cr catalysts both in the presence and absence of CO. A comparison of catalyst activities is shown in Fig. 4. Three conversion versus temperature profiles are shown for each catalyst: (1) methanol conversion in a feed containing $CH_3OH$ and $O_2$ (solid curve), (2) methanol conversion in a feed containing $CH_3OH$, CO, and $O_2$ (dash-dot-curve) and (3) CO conversion in a feed containing CO and $O_2$ (dotted curve). The behavior of the noble metal catalysts, Pt and Pd, contrasted with that of the base metal catalysts, Ag and Cu-Cr. $CH_3OH$ oxidation was strongly inhibited over the Pt and Pd catalysts by the addition of CO to the feed. This is demonstrated by the 100-150° shift of the $CH_3OH$ conversion profiles to higher temperatures in the presence of added CO.[3] Additionally, the $\underline{CH_3OH}$ conversion profiles observed in the presence of CO superposed almost exactly on the $\underline{CO}$ oxidation profiles, indicating that $CH_3OH$ oxidation is totally dominated by CO oxidation on the Pt and Pd catalysts. This is not unexpected given that CO adsorbs much more strongly on Pt and Pd surfaces than $CH_3OH$ [4-7], and $CH_3OH$ cannot adsorb and react until temperatures are reached where CO begins to desorb.

In contrast to Pt and Pd, CO chemisorption on Ag and Cu-Cr catalysts is very weak [8-14]. Consequently, CO oxidation activities of the Ag and Cu-Cr catalysts are poor compared to Pt and Pd. Because of the weak CO adsorption, however, adsorption and reaction of $CH_3OH$ are not inhibited by CO as in the case of the noble metal catalysts. Thus, the methanol conversion profiles shown for the Ag and Cu-Cr catalysts in Fig. 4. are virtually unaffected by the presence of CO.

### Motivations for Utilizing Bimetallic Catalysts

Comparison of the $CH_3OH$ oxidation data of Figs. 4a and 4d, for the Pt and Ag catalysts respectively, indicates that, in the presence of CO, $CH_3OH$ oxidation proceeds more readily on the Ag catalyst at low temperatures than on the Pt catalyst. This comparison is shown more clearly in Fig. 5 where the methanol conversion profiles obtained in the presence of CO are plotted

together. The Ag catalyst is more active at low temperatures (hashed region), but the curves cross at high temperatures. Together, these observations suggest that a bimetallic catalyst containing Ag in combination with either Pt or Pd would show better $CH_3OH$ oxidation activity over the full range of temperatures in automotive exhaust than either Ag, Pt, or Pd catalysts alone.

A bimetallic catalyst such as Pd-Ag might also prove to be a more efficient low-temperature CO oxidation catalyst than the respective single-component catalysts. The basis for this suggestion is shown conceptually in Fig. 6. At low temperatures, CO oxidation rates are low on Pd catalysts because of the high surface coverage of CO which prevents $O_2$ adsorption. Ag represents the other extreme; CO interacts only weakly with Ag thus its surface coverage is low. A catalyst containing Pd and Ag, intimately mixed in bimetallic crystallites, might promote CO oxidation by effecting more-uniform surface concentrations of CO and atomic oxygen than can be obtained with either Pd or Ag alone.

## Design of a Pd-Ag Catalyst

A Pd-Ag/$Al_2O_3$ catalyst was prepared utilizing a strategy designed to disperse small amounts of Pd over much larger amounts of Ag. The Ag loading was 5% by weight. This loading was chosen because, as shown in Fig. 7, CO conversion activity was found to depend strongly on Ag loading. In contrast, CO conversion activity over Pd catalysts (Fig. 8) did not depend strongly on loading under the conditions of our study. Thus a low loading of 0.01% was chosen and uniform impregnation techniques were employed to highly disperse the Pd and thereby avoid the formation of segregated Pd particles.

Details of the methanol oxidation behavior of the bimetallic catalyst have been reported elsewhere [15]. The activity characteristics and selectivity patterns confirm that the preparative techniques outlined above produce a catalyst where essentially all of the Pd is present in bimetallic crystallites rather than as segregated Pd particles.

## CO Oxidation over the Pd-Ag Catalyst

The CO oxidation activity of the 0.01% Pd-5% Ag catalyst was compared to the CO oxidation activities of 0.01% Pd and 5% Ag catalysts alone. Fig. 9 shows data obtained at a space velocity of 195,000 $h^{-1}$. At temperatures below 500 K, the Pd-Ag catalyst showed higher CO conversions than either of the single-component catalysts. Moreover, the shape of the conversion versus temperature profile closely resembled that of the Ag catalyst, which suggests that the role of Pd in the bimetallic catalyst is to promote CO oxidation on Ag.

CO oxidation was also examined at a space velocity of 52,000 $h^{-1}$, and results are shown in Fig. 10. In contrast to the data obtained at 195,000 $h^{-1}$, the Pd-Ag catalyst showed enhanced conversion relative to the Ag catalyst only at temperatures above ~450 K.

## Mechanism of Pd Promotion of the Ag Catalyst

The addition of Pd to the Ag catalyst has an effect that is similar to increasing the feed oxygen concentration over an Ag catalyst. This can be seen by comparing Figs. 10 and 11. In Fig. 11, $CH_3OH$ oxidation data are shown for a 2% $Ag/Al_2O_3$ catalyst at two oxygen concentrations. At low temperatures, $CH_3OH$ conversions are virtually identical, indicating that the rate of $O_2$ supply is not a limiting factor. At temperatures above 400 K, however, the curves diverge. $CH_3OH$ conversion is greater in the 1% $O_2$ feed than in the 0.25% $O_2$ feed, as expected under conditions where the overall reaction rate increases to the point where the supply of oxygen becomes a rate-determining step. Since the same qualitative behavior is observed in comparing CO oxidation over the Pd and Pd-Ag catalysts in Fig. 10 the data suggest that the effect of adding small amounts of Pd to an Ag catalyst is to increase the rate of $O_2$ adsorption and subsequent reaction on the Ag.

Fig. 12 shows results of temperature-programmed oxidation (TPO) experiments carried out over pre-reduced samples of the 0.01% Pd, 5% Ag, and 0.01% Pd-5% Ag catalysts. The TPO experiments provide additional evidence that the role of Pd in the bimetallic catalyst is to increase the rate of $O_2$ adsorption and reaction on Ag. No $O_2$ adsorption was observed on the 0.01% Pd catalyst due to the very low metal loading (any $O_2$ uptake associated with the 0.01% Pd catalyst would have been below the sensitivity of the thermal conductivity detectors employed in the TPO apparatus). However, the Pd-Ag catalyst showed greater rates of $O_2$ uptake than the Ag catalyst alone at temperatures below 600 K. The enhanced uptake rate of the Pd-Ag catalyst indicates that Pd enhances the rate of $O_2$ adsorption on the Ag, since as noted previously, any uptake associated with Pd was below the limits of detectability. This observation is consistent with the relatively high sticking probabilities reported for dissociative $O_2$ chemisorption on Pd surfaces ($s_o$ ~$10^{0}$-[16])[4] compared to the extremely low values reported for Ag surfaces ($s_o$ = $10^{-6}$-$10^{-4}$ [17, 18]).

## SUMMARY

Although a synergistic interaction between Pd and Ag has been achieved in this study, the enhanced rates of CO and $CH_3OH$ oxidation result from Pd promoting the rate of $O_2$ adsorption and reaction on Ag, rather than from a bifunctional mechanism.

In other words, our data suggest that both CO and $CH_3OH$ oxidation occur nearly exclusively on Ag in the bimetallic catalyst with the role of Pd being to supply oxygen atoms at a rate greater than that of direct dissociative $O_2$ adsorption on Ag crystallites. This is in contrast to the situation depicted in Fig. 6, where the synergism would result from adsorption of CO and Ag on the different metal components in close proximity.

Thus, in this study, the bimetallic catalyst shows its greatest rate enhancement relative to the single-component catalysts under conditions where the surface reactions are fast relative to the rate of $O_2$ adsorption. These are not the conditions that would obtain in a low-temperature $CO_2$ laser application. The surface reaction between adsorbed CO and adsorbed atomic oxygen would likely be rate-limiting, and multimetallic catalysts that adsorb CO and $O_2$ independently on adjacent sites would appear to offer the greatest rate enhancement.

This sort of configuration has, in fact, been suggested for the structure of Pt-$SnO_x$ catalysts where Pt-O-Sn bonding has been identified. This bonding configuration could represent the active sites for CO and O adsorption and reaction, thereby eliminating the requirement for surface diffusion of either species [19].

## REFERENCES


1. R. W. McCabe and P. J. Mitchell, Applied Catalysis 27 (1986) 83.

2. S. R. Seyedmonir, D. E. Strohmayer, G. L. Geoffroy, M. A. Vannice, H. W. Young, and J. W. Linowski, J. Catalysis 87 (1984) 424.

3. S. R. Seyedmonir, D. E. Strohmayer, G. J. Guskey, G. L. Geoffroy, and M. A. Vannice, J. Catalysis 93 (1985) 288.

4. R. K. Herz and S. P. Marin, J. Catalysis 65 (1980) 281.

5. A. Golchet and J. M. White, J. Catalysis 53 (1978) 266.

6. R. W. McCabe and L. D. Schmidt, Surface Sci. 66 (1977) 101.

7. B. A. Sexton, Surface Sci. 102 (1981) 271.

8. R. J. Madix, In "Advances in Catalysis," Academic Press: New York, 1980.

9. C. R. Ryberg, Phys. Rev. Lett. 49 (1982) 1579.

10. T. E. Felter, W. H. Weinberg, G. Ya. Lastushkina, P. A. Zndan, G. K. Boreskov, and J. Hrbek, Appl. Surf. Sci. 16 (1983) 351.

11. I. E. Wachs and R. J. Madix, Surface Sci. 76 (1978) 53.

12. R. Hierl, H. Knozinger, and H.-P. Urbach, J. Catalysis 69 (1981) 475.

13. M. Ayyoob and M. S. Hegde, Surface Sci. 133 (1983) 516.

14. H. Albers, W. J. J. Vander Wal and G. A. Bootsma, Surface Sci. 68 (1977) 47.

15. R. W. McCabe and P. J. Mitchell, J. Catalysis 103 (1987).

16. H. Conrad, G. Ertl, J. Kuppers, and E. E. Latta, Surface Sci. 65 (1977) 245.

17. C. T. Campbell, Surface Sci. 157 (1985) 43; and references therein.

18. H. Albers, N. J. Vander Wal, O. L. J. Gijzeman and G. A. Bootsma, Surface Sci. 77 (1978) 1.

19. G. B. Hoflund and D. A. Asbury, "Thin Solid Films," 129 (1985) 139.

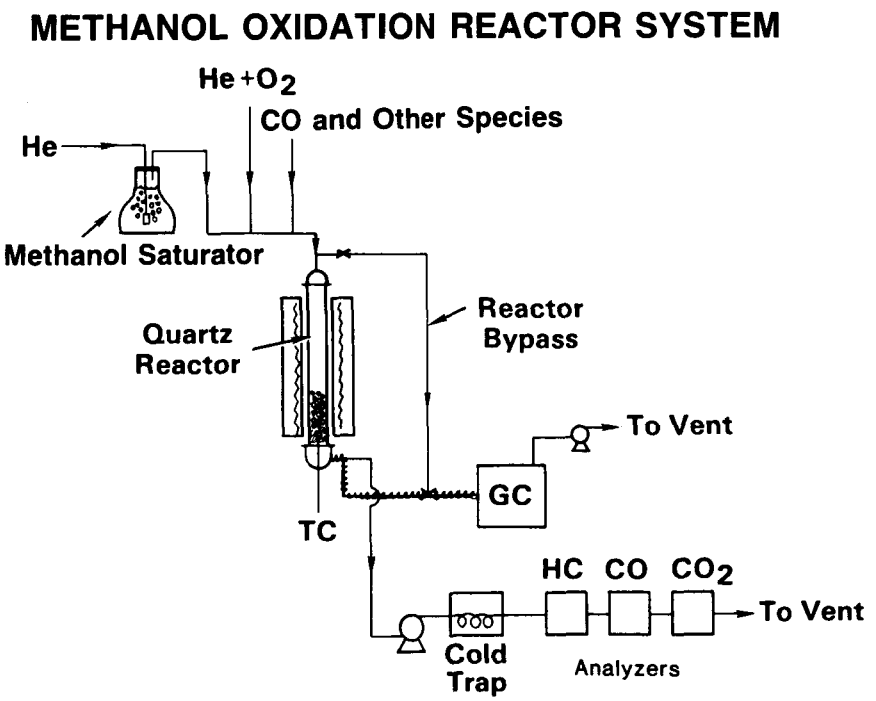


Figure 1. Schematic diagram of reactor apparatus.

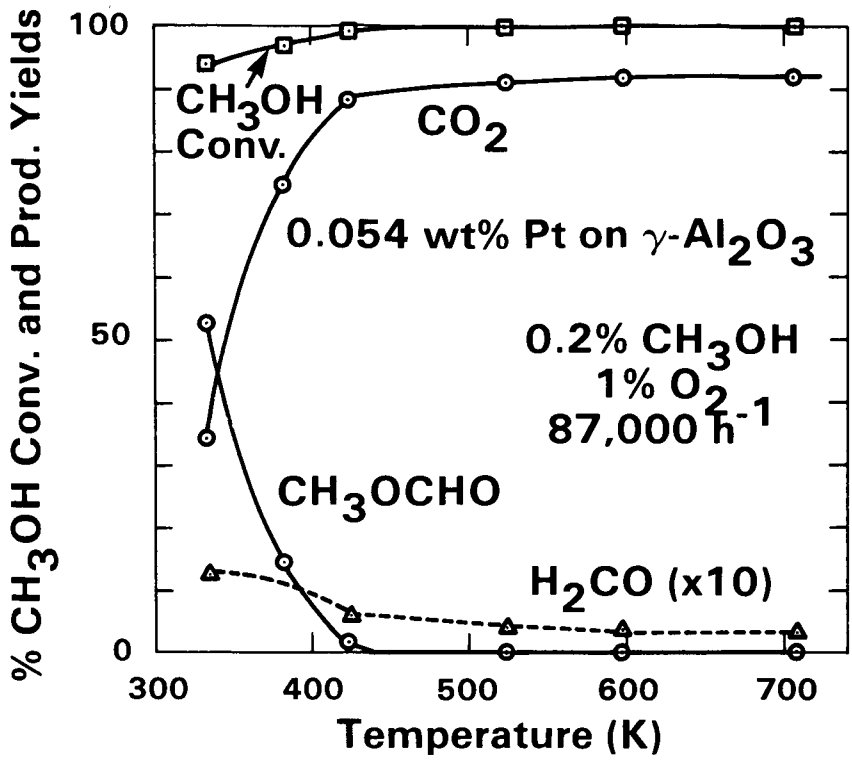


Figure 2. Steady-state methanol conversions and product yields as a function of temperature over a 0.054 wt% $Pt/Al_2O_3$ catalyst.

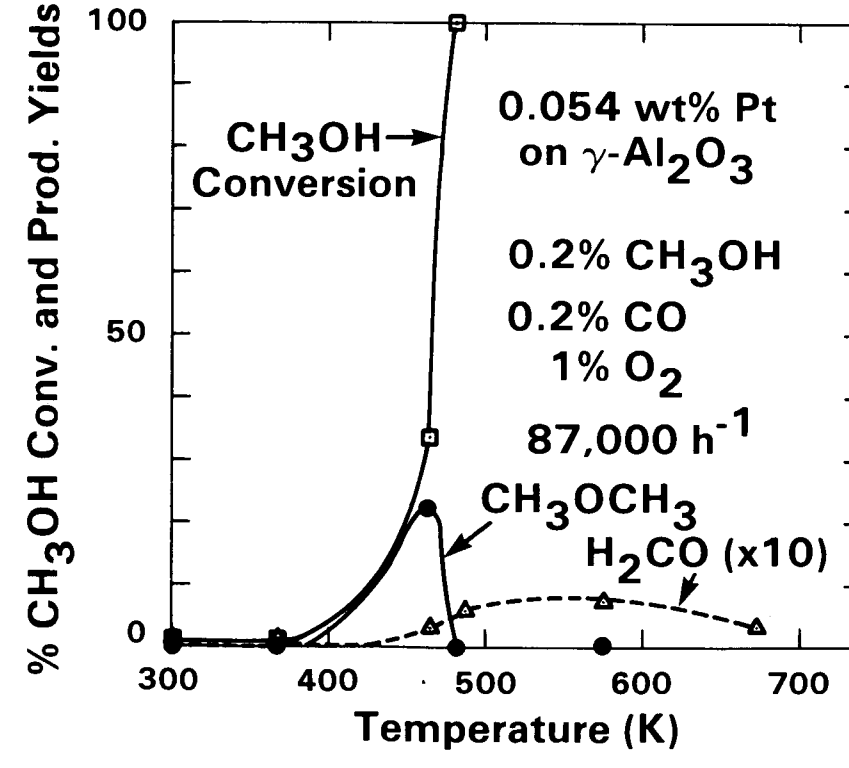


Figure 3. Steady-state methanol conversions and product yields as a function of temperature over a 0.054 wt% $Pt/Al_2O_3$ catalyst. The experiment was identical to that of Fig. 2 except that 0.2% CO was added to the feed.

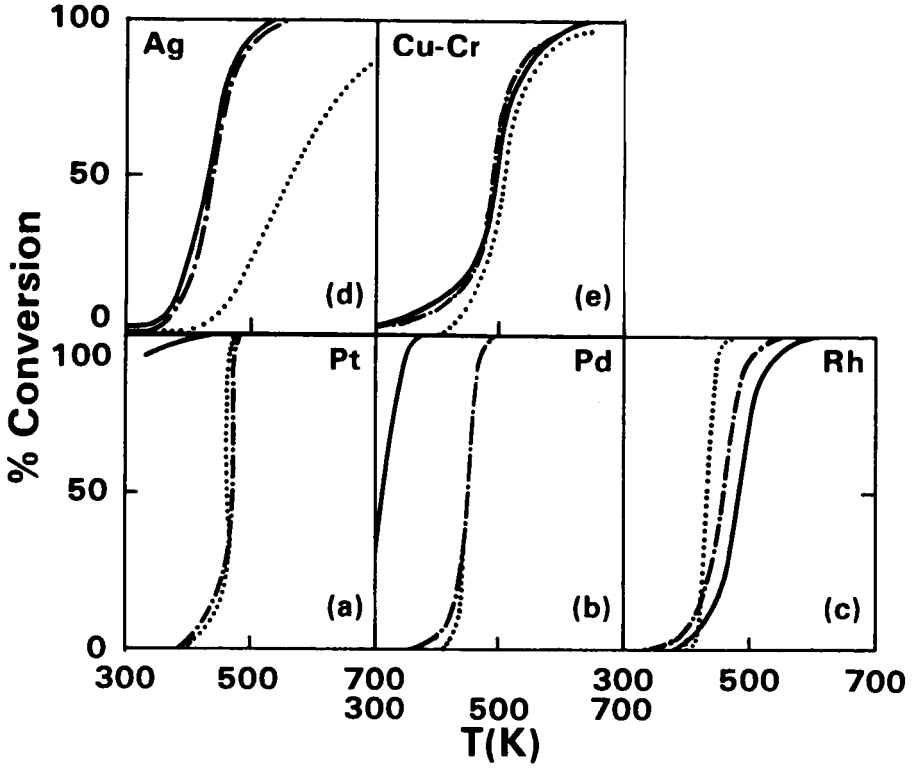


Figure 4. A comparison of conversion versus temperature data obtained over (a) 0.054 wt% Pt, (b) 0.034 wt% Pd, (c) 0.026 wt% Rh, (d) 1.92 wt% Ag, and (e) 4 wt% Cu-2 wt% Cr all supported on $\gamma$-$Al_2O_3$. For each catalyst we show conversion vs temperature data for feeds containing (1) 0.2% $CH_3OH$/1% $O_2$ (----), (2) 0.2% CO/1% $O_2$ (....) and (3) 0.2% $CH_3OH$/0.2% CO/1% $O_2$ (--•--). For the mixed 0.2% $CH_3OH$/0.2% CO/1% $O_2$ feed, the conversion reported is that of $CH_3OH$, not CO.

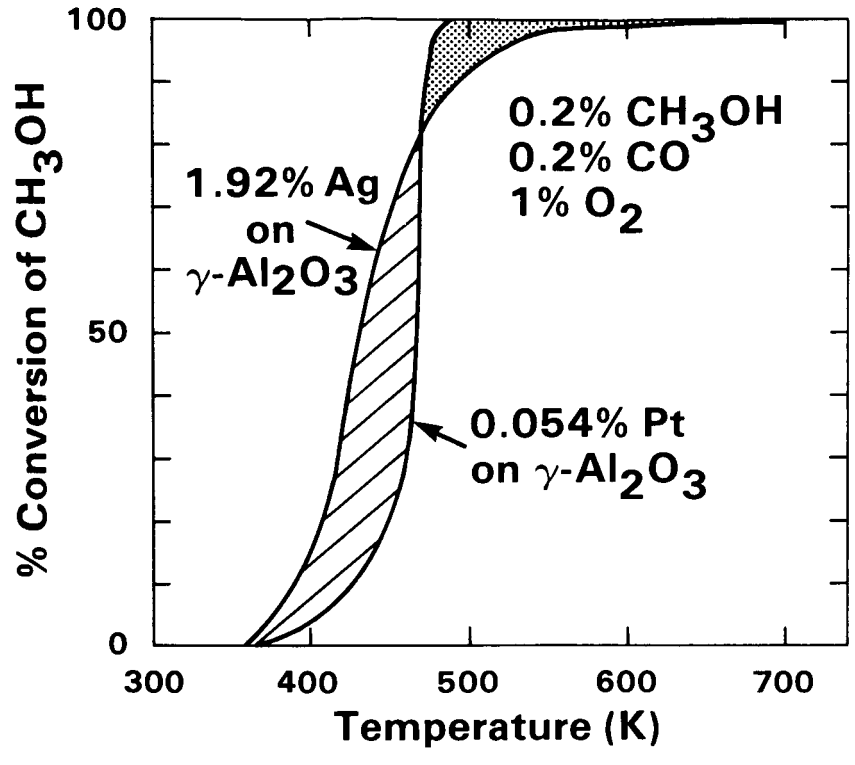


Figure 5. A comparison of methanol conversions over 2 wt% Ag and 0.054 wt% Pt catalysts as a function of temperature.

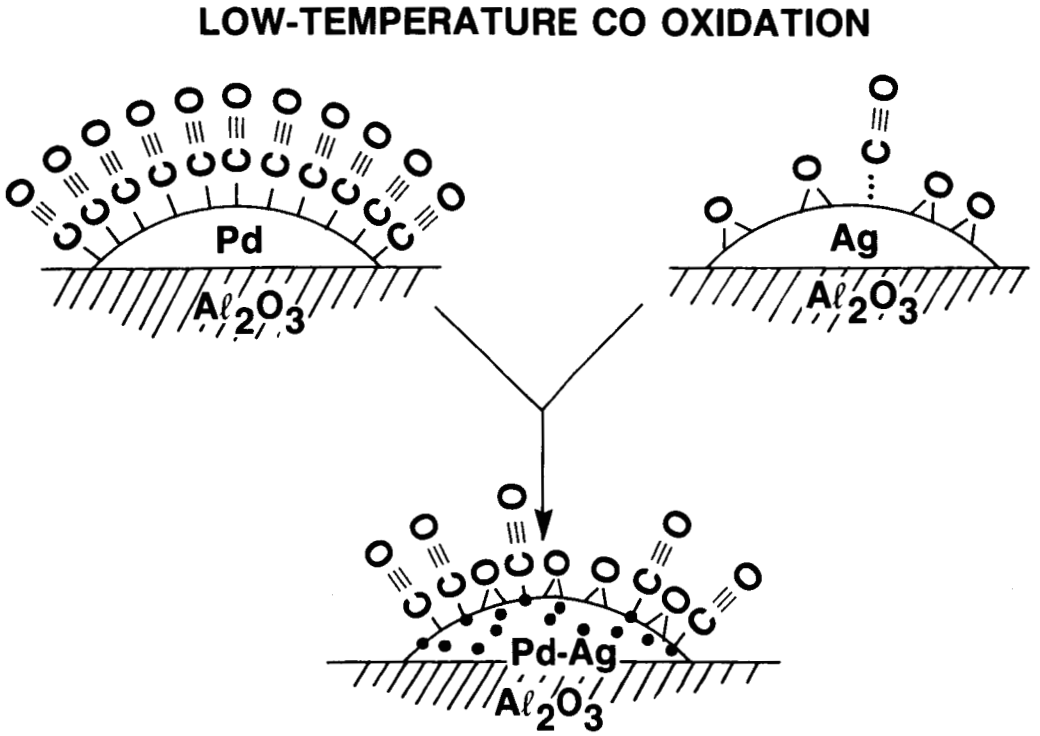


Figure 6. A conceptual representation of surface coverages of adsorbed species expected for CO oxidation on alumina-supported Pd, Ag, and Pd-Ag catalysts at low temperatures. The bimetallic catalyst would be expected to result in a more uniform surface mixture of CO and O than either of the single-component catalysts.

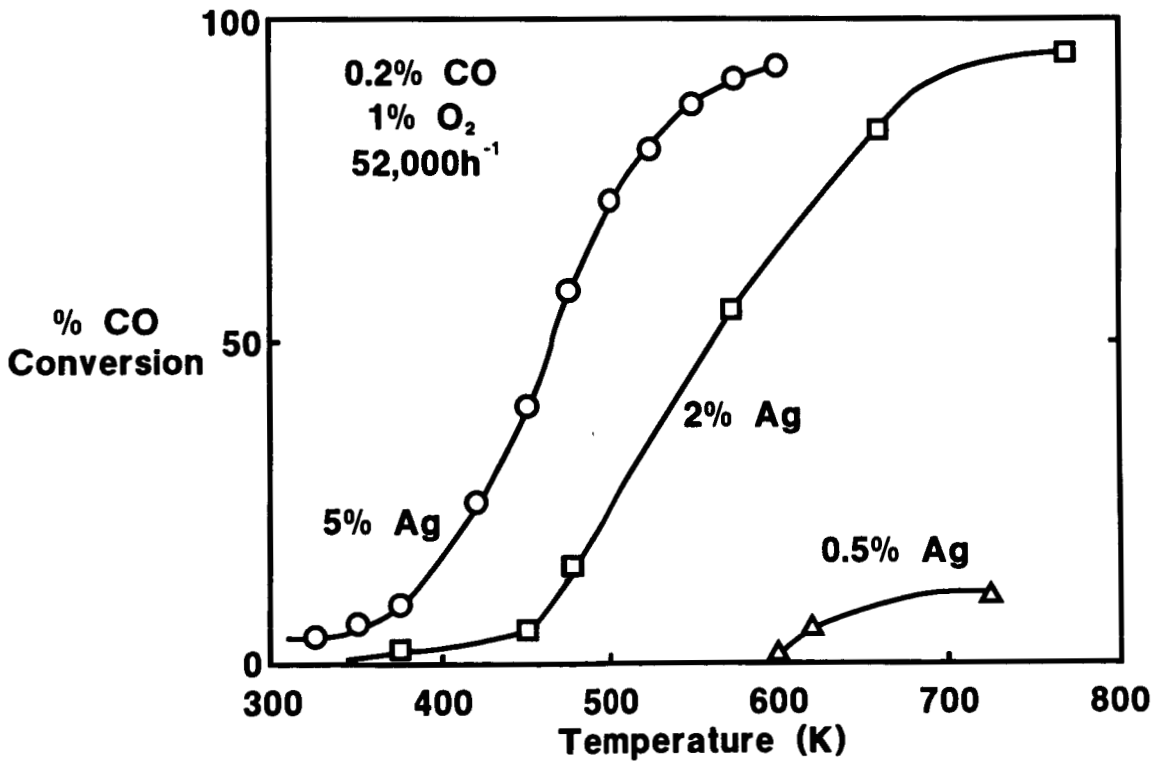


Figure 7. Effect of loading on Ag/γ-$Al_2O_3$ catalyst CO oxidation activity.

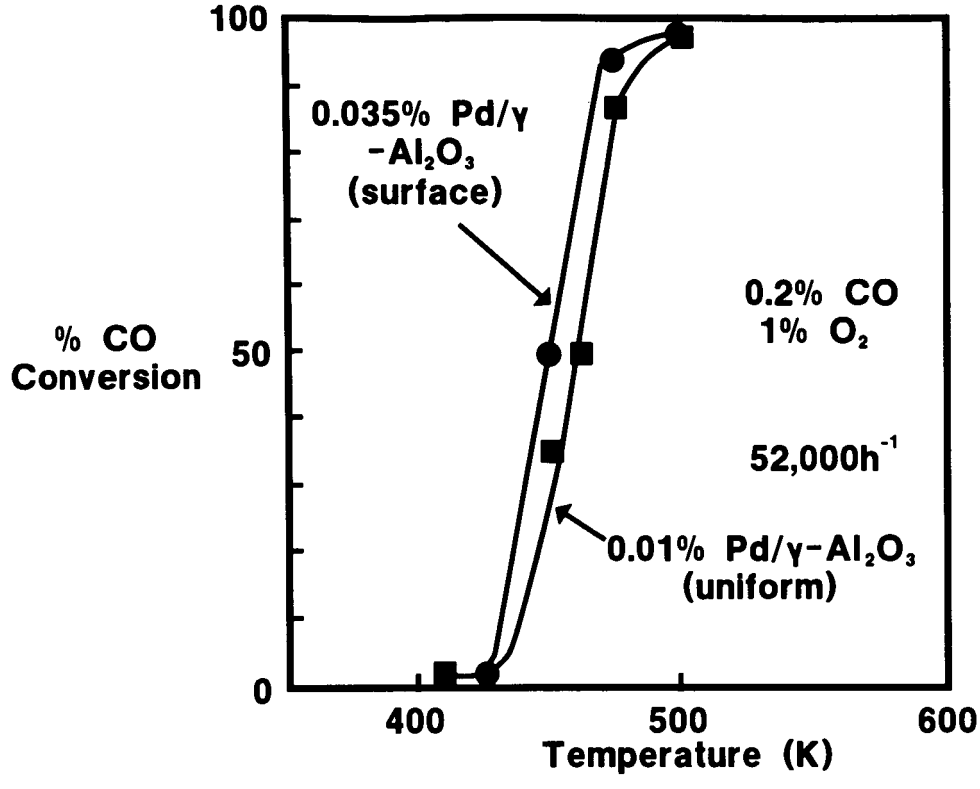


Figure 8. Comparison of CO oxidation activities of two Pd/Y-$Al_2O_3$ catalysts.

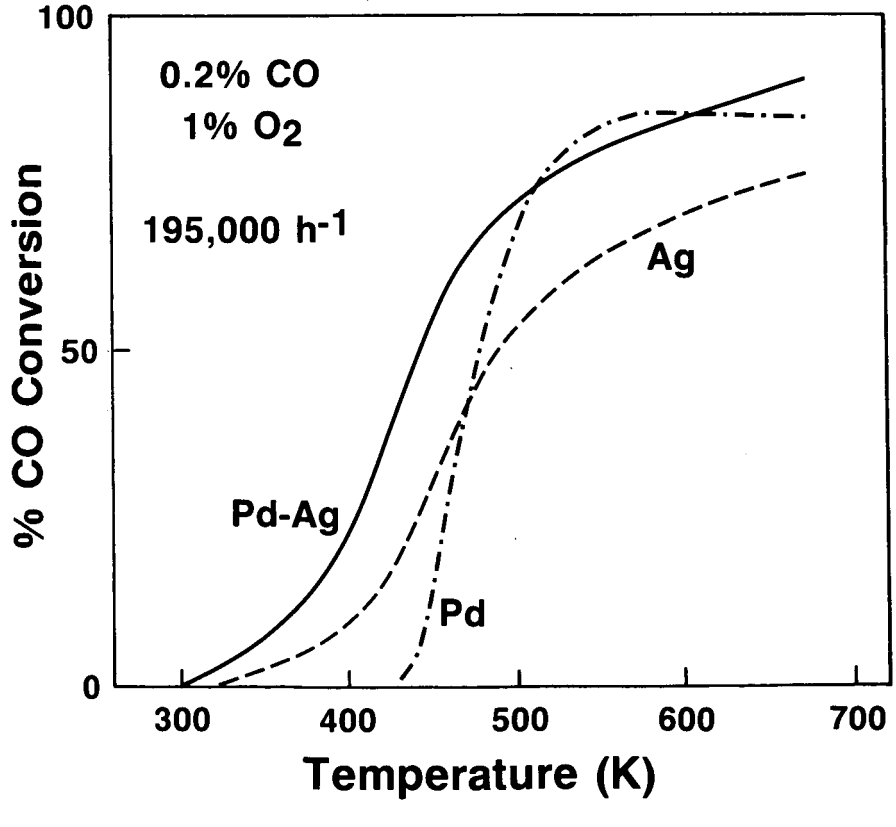


Figure 9. Conversion as a function of temperature for CO oxidation at 195,000 $h^{-1}$ over 0.01 wt% Pd, 5 wt% Ag, and 0.01 wt% Pd-5 wt% Ag alumina-supported catalysts.

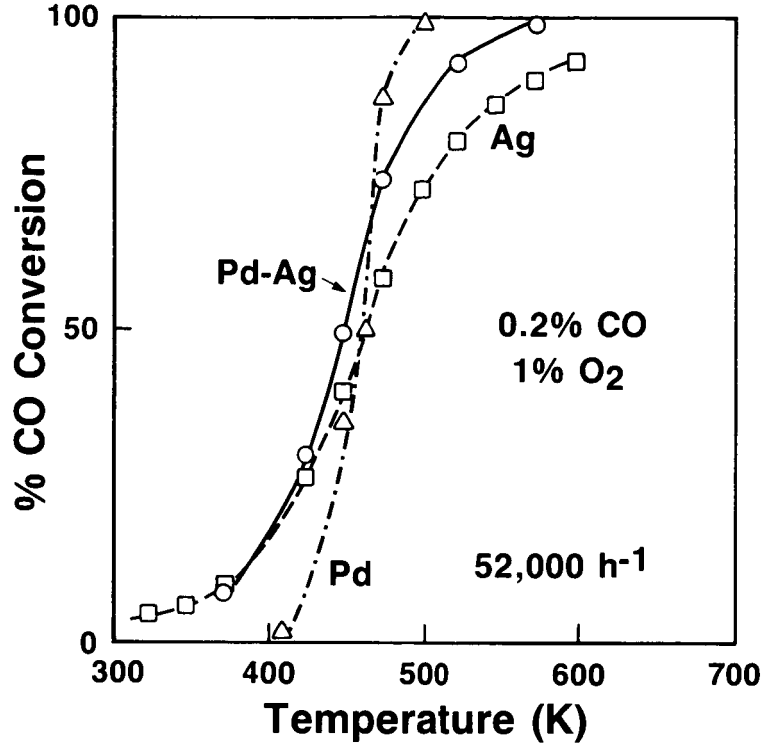


Figure 10. Conversion as a function of temperature for CO oxidation at 52,000 $h^{-1}$ over 0.01 wt% Pd, 5 wt% Ag, and 0.01 wt% Pd-5 wt% Ag alumina-supported catalysts.

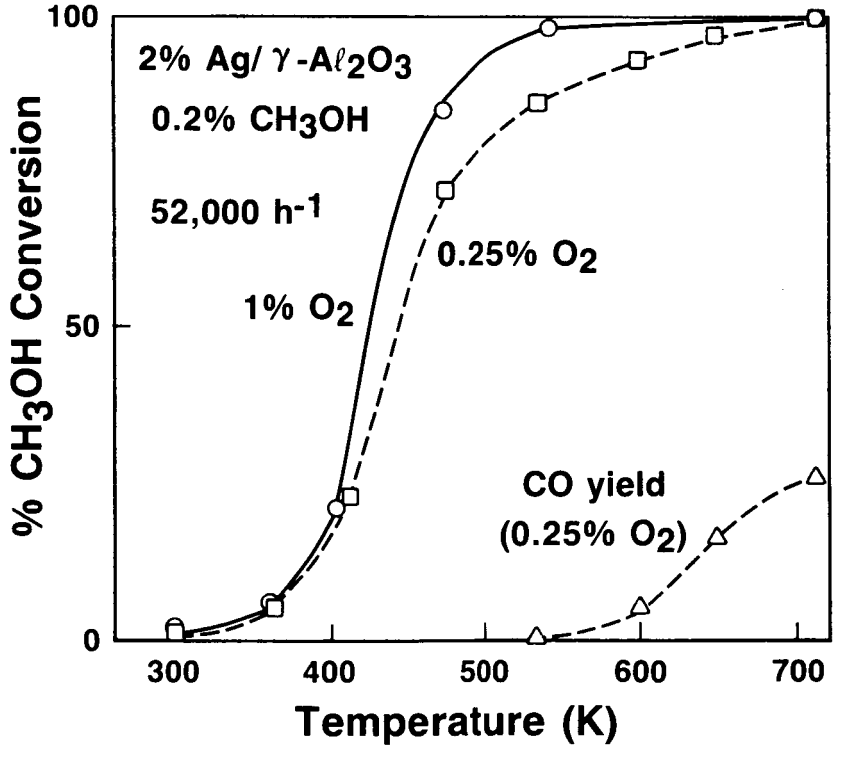


Figure 11. Effect of feed $O_2$ concentration on $CH_3OH$ conversion profiles obtained over a 2 wt% $Ag/Al_2O_3$ catalyst.



C-3

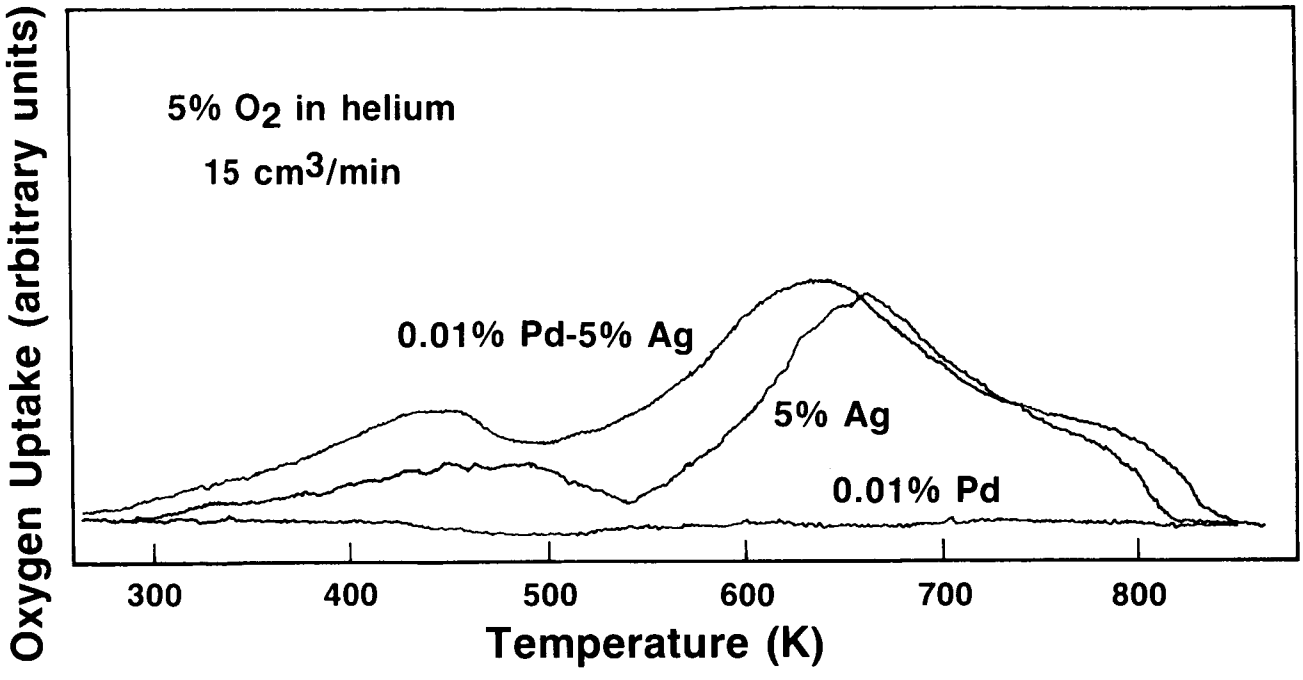


Figure 12. Temperature-programmed oxidation profiles for pre-reduced samples of 0.01 wt% Pd, 5 wt% Ag, and 0.01 wt% Pd-5 wt% Ag catalysts.